



Sphingolipid extracts enhance gene delivery of cationic lipid vesicles into retina and brain

Nuseibah AL Qtaish^{a,b,1}, Idoia Gallego^{a,b,c,1}, Ilia Villate-Beitia^{a,b,c}, Myriam Sainz-Ramos^{a,b,c}, Gema Martínez-Navarrete^{b,d}, Cristina Soto-Sánchez^{b,d}, Eduardo Fernández^{b,d}, Patricia Gálvez-Martín^e, Tania B. Lopez-Mendez^{a,b,c}, Gustavo Puras^{a,b,c,*}, José Luis Pedraz^{a,b,c,*}

^a NanoBioCel Research Group, Laboratory of Pharmacy and Pharmaceutical Technology. Faculty of Pharmacy, University of the Basque Country (UPV/EHU), Paseo de la Universidad 7, 01006 Vitoria-Gasteiz, Spain

^b Networking Research Centre of Bioengineering, Biomaterials and Nanomedicine (CIBER-BBN), Institute of Health Carlos III, Av Monforte de Lemos 3-5, 28029 Madrid, Spain

^c Bioaraba, NanoBioCel Research Group, Calle José Ahotegui s/n, 01009 Vitoria-Gasteiz, Spain

^d Neuroprosthesis and Neuroengineering Research Group, Institute of Bioengineering, Miguel Hernández University, Avenida de la Universidad, 03202 Elche, Spain

^e R&D Human Health, Bioibérica S.A.U., Plaza Francesc Macià, 08029 Barcelona, Spain

ARTICLE INFO

Keywords:

Gene therapy
Niosomes
Niosphingosomes
Sphingolipids
Brain
Retina

ABSTRACT

The aim was to evaluate relevant biophysic processes related to the physicochemical features and gene transfection mechanism when sphingolipids are incorporated into a cationic niosome formulation for non-viral gene delivery to central nervous system. For that, two formulations named niosphingosomes and niosomes devoid of sphingolipid extracts, as control, were developed by the oil-in water emulsion technique. Both formulations and the corresponding complexes, obtained upon the addition of the reporter EGFP plasmid, were physicochemically and biologically characterized and evaluated. Compared to niosomes, niosphingosomes, and the corresponding complexes decreased particle size and increased superficial charge. Although there were not significant differences in the cellular uptake, cell viability and transfection efficiency increased when human retinal pigment epithelial (ARPE-19) cells were exposed to niosphingoplexes. Endocytosis via caveolae decreased in the case of niosphingoplexes, which showed higher co-localization with lysosomal compartment, and endosomal escape properties. Moreover, niosphingoplexes transfected not only primary central nervous system cells, but also different cells in mouse retina, depending on the administration route, and brain cortex. These preliminary results suggest that niosphingosomes represent a promising non-viral vector formulation purposed for the treatment of both retinal and brain diseases by gene therapy approach.

1. Introduction

Gene therapy is an arising medical option for treating inherited and acquired diseases, which has captured the interest and investment of many pharmaceutical companies during the last few years [1]. Its main

concept lays on the delivery of foreign genetic material into target cell in order to correct a specific pathology [2]. However, the regular practice of this advanced technology needs to surpass many biological extracellular barriers in order to reach the target cells, which depends on both the organ/cell type to be treated and the route of administration [3].

Abbreviations: Arpe-19, human retinal pigment epithelial cells; BBB, blood-brain-barrier; BRB, blood-retinal-barrier; BSA, bovine serum albumin; CCF, cross-correlation function; CME, clathrin mediated endocytosis; CvME, caveolae mediated endocytosis; DCM, dichloromethane; DMEM/F12, Dulbecco's Modified Eagle.

* Corresponding authors at: Laboratory of Pharmacy and Pharmaceutical Technology. Faculty of Pharmacy, University of the Basque Country, Paseo de la Universidad 7, 01006 Vitoria-Gasteiz, Spain.

E-mail addresses: nhasanflayyeh002@ikasle.ehu.es (N. AL Qtaish), idoia.gallego@ehu.es (I. Gallego), aneilia.villate@ehu.es (I. Villate-Beitia), miriam.sainz@ehu.es (M. Sainz-Ramos), gema.martinez@umh.es (G. Martínez-Navarrete), csoto@goumh.umh.es (C. Soto-Sánchez), e.fernandez@umh.es (E. Fernández), pgalvez@bioiberica.com (P. Gálvez-Martín), tania.lopez@ehu.es (T.B. Lopez-Mendez), gustavo.puras@ehu.es (G. Puras), joseluis.pedraz@ehu.es (J. Luis Pedraz).

¹ N. AL Qtaish and Dr. I. Gallego contributed equally to this work.

<https://doi.org/10.1016/j.ejpb.2021.09.011>

Received 20 July 2021; Received in revised form 23 September 2021; Accepted 27 September 2021

Available online 2 October 2021

0939-6411/© 2021 The Authors.

Published by Elsevier B.V. This is an open access article under the CC BY-NC-ND license

(<http://creativecommons.org/licenses/by-nc-nd/4.0/>).

This fact is mostly relevant in the case of immune-privileged organs, which are isolated from the rest of the organism by the blood–brain-barrier (BBB) and the blood-retinal-barrier (BRB), such as brain and retina, respectively [4,5]. Moreover, to be biologically effective, it is necessary to deliver enough genetic material inside target cells. In this sense, the endocytosis mechanism and the following intracellular trafficking process clearly affects the final disposition of the genetic material at the place of action [6]. Therefore, in order to overcome both extracellular and intracellular barriers, safe and effective gene delivery systems need to be developed [7].

Research on the design, development and application of non-viral vectors has considerably increased during the last years to enhance gene delivery efficiency [8]. Among the different kinds of non-viral vectors, those related to cationic lipids are the most studied ones [9]. In fact, Pfizer/BioNTech and Moderna companies, with the approval of regulatory agencies, have recently applied this lipid based-technology to formulate mRNA vaccines to face the devastating Covid-19 disease. Any slight variation in the composition of these lipid structures can impact on both the physicochemical properties and the gene delivery capacity [10]. In order to increase the biophysical activity, such cationic lipids are normally incorporated into colloidal vesicles made up of phospholipids, leading to the formation of the corresponding liposomes [11]. If cationic lipids are combined with non-ionic surfactant components to enhance chemical stability, a colloidal dispersion of niosomes is obtained [12]. Such niosomes have been recognized during last years to deliver efficiently and safely the genetic material for different applications [13]. In addition to cationic lipid and the non-ionic surfactant, other chemical agents referred as “helper” compounds can also be incorporated into the niosome vesicles to enhance their biological performance [14]. Some compounds that have been successfully incorporated into niosomes as “helper” components include cholesterol [15], squalene [16], lycopene [17] or chloroquine [18], to name just a few.

Sphingolipids are biomaterials referred as a class of natural complex lipids mainly found in membranes of the central nervous system tissue, which play a relevant biological role in cell signaling processes [19]. Such sphingolipids derive from sphingosine, an alkalonamide of 18 carbons. Sphingolipids are obtained when a long saturated or unsaturated fatty acid chain is bound to the amino reactive group and another radical consisting of *phosphocholine* or sugar, binds to the final carboxylic group of the sphingosine, resulting in the formation of ceramides [20]. Sphingolipid extracts can be obtained from animals, plants, and can also be produced from genetically modified microorganisms. However, in mammals, endogenous sphingolipids contain high levels of sphingosine, which is not present in extracts from plants or in sphingolipids obtained from microorganisms. Therefore, sphingolipid extracts obtained from animal origin show a more suitable lipid profile to obtain ceramides [21]. It has been suggested that glycosphingolipids might be involved in the transmembrane transport and binding of bacteria and bacterial toxins to intestinal epithelial cells. Besides, the composition of glycolipids in the rat small intestinal mucosa demonstrated alterations during normal differentiation and development, pointing to possible roles for glycosphingolipids in these processes as well [22].

Sphingolipids have been successfully incorporated as structural components into different nanocarrier systems for drug delivery purposes [23–25]. However, currently, there is not any report related to the use of such sphingolipids on the transfection process mediated by cationic niosomes. Therefore, to address such issue, we performed a comparative study of two non-viral vector formulations based on cationic niosomes consisting of the same cationic lipid and non-ionic tensioactive, but with or without sphingolipids as “helper” compound, obtaining niosomes or niosomes, respectively. Both formulations were developed by the oil-in water (o/w) emulsion technique, and the corresponding complexes obtained after the addition of the EGFP reporter plasmid at different cationic lipid/DNA ratios (w/w) were physicochemically characterized before performing transfection

experiments in ARPE-19 cells to evaluate cell viability, gene expression, cellular uptake and intracellular trafficking. Preliminary *in vivo* experiments were carried out to evaluate gene expression of the most promising complexes in rat brain, after cerebral cortex injection, and in rat retina, after both intravitreal and subretinal administration.

2. Materials and methods

2.1. Preparation of formulations

The cationic formulations were developed by the o/w emulsion technique. The 1, 2-di-O-octadecenyl-3-trimethylammonium propane chloride salt (DOTMA, Avanti Polar Lipids, Inc., Alabama, USA) cationic lipid, in combination with 2-2-3, 4-bis(2-hydroxyethoxy oxolan-2-yl)-2-2-hydroxyethoxy ethoxy ethyl dodecanoate (Tween 20, Bio-Rad, Madrid, Spain) non-ionic surfactant, were mixed or not with sphingolipids from animal origin found in the intestinal mucosa of mammal, which had a 63% percentage of sphingomyelin content (Bioiberica laboratory, *Sus scrofa*, pig), as helper components, obtaining niosomes and niosomes, respectively (Fig. 1). Briefly, the cationic lipid (3.4 mg) was gently grounded with sphingolipids (100 µg), then, dichloromethane (DCM) (500 µL) (Panreac, Barcelona, Spain) was added to this lipid mixture and emulsified with the non-ionic surfactant aqueous solution of polysorbate 20 (2.5 mL) (0.5%, w/v). Components were sonicated (Branson Sonifier 250, Danbury) for 30 s at 50 W. Next, the DCM organic solvent was evaporated and eliminated from the emulsion by using magnetic stirrer for 2 h at room temperature inside a extraction hood. Upon DCM evaporation, a colloidal dispersion containing the formulations was obtained with a final cationic lipid concentration of 1.5 mg mL⁻¹.

2.2. Plasmid propagation and complexes elaboration

The pCMS-EGFP plasmid (Plasmid Factory, Bielefeld, Germany) was propagated with *Escherichia coli* DH5-α and purified as previously described [15]. The stock solution of plasmid pCMS-EGFP (0.5 mg mL⁻¹) was estimated to be around 0.137 µM (pCMS-EGFP, 5541 bp, average MW 3657060 g mol⁻¹).

Complexes were formed by adding an appropriate volume of the plasmid to either niosomes or niosomes at different cationic lipid/DNA mass ratios (w/w). The mixture was incubated for 30 min at room temperature before use to promote the electrostatic interactions between the amine groups of the cationic lipid and the phosphate groups of the genetic material to obtain the resulting complexes.

2.3. Physicochemical characterization of formulations

The hydrodynamic diameter of nanoparticles was recorded to report the particle size by dynamic light scattering, and laser doppler velocimetry was used to determine zeta potential, using Zetasizer Nano ZS (Malvern Instrument, UK) as previously described [15]. All measurements were performed in triplicate. Transmission electron microscopy (TEM) was used to define the morphology of formulations, as previously described [12].

2.4. Qualitative analysis of the transfection efficiency and cellular uptake

To evaluate the transfection efficiency qualitatively, ARPE-19 cells were seeded into 24 well plates at an initial density of 18 × 10⁴ cells per well, to reach 70–80% of confluence at the time of transfection assay. Next, cells were exposed to formulations containing EGFP (1.25 µg) plasmid per well during 4 h in OptiMEM® transfection medium (Gibco®, Life Technologies, S.A., Madrid, Spain). Afterwards, OptiMEM® was replaced by DMEM/F-12 regular growth medium (Gibco®, Life Technologies, S.A., Madrid, Spain) containing 10% bovine serum, and cells were allowed to grow for 48 h until their observation under

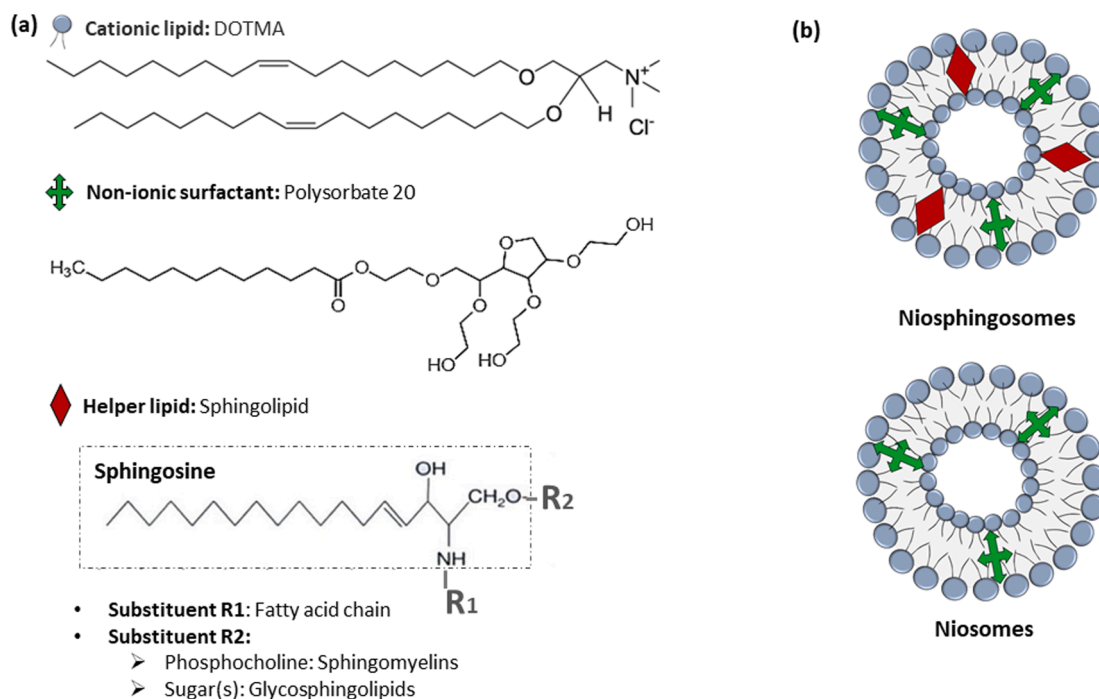


Fig. 1. Scheme of composition of niosphingosomes and niosomes. (a) General chemical structure of cationic lipid, non-ionic surfactant and helper component. (b) General scheme showing the disposition of the components in the formulations of both niosphingosomes and niosomes.

fluorescence microscopy. Images showing EGFP signal in ARPE-19 cells transfected with niosphingoplexes and nioplexes were captured at this time. To evaluate cellular uptake, cells were processed, fixed and analyzed as previously described [26].

2.5. Quantitative analysis of EGFP expression, cell viability and cellular uptake

FACSCalibur flow cytometer (Becton Dickinson Bioscience, San Jose, USA) was used to perform flow cytometry analysis in order to quantify the percentage of EGFP and FITC-labeled EGFP plasmid (Dare Bioscience) expression for transfection and cellular uptake assays, respectively. For this purpose, at the end of incubation time, which was 48 h for transfection assay and both 2 h and 4 h for cellular uptake assay, cells were washed with PBS (Gibco™, San Diego, California, USA) and detached from the 24 wells with trypsin/EDTA (200 μ L) (Gibco™, San Diego, California, USA). Then, cells were prepared and analyzed as previously described [15].

2.6. Endocytic trafficking

Cells were seeded in 24 well plates with coverslips at an initial density of 18×10^4 cells per well and incubated at 37 °C with 5% CO₂ atmosphere to reach 70–80% of confluence at the time of internalization assay. Next, cells were exposed to formulations containing EGFP plasmid (1.25 μ g per well) during 3 h in OptiMEM® transfection medium and endocytic fluorescent markers for 1 h at 37 °C and 5% CO₂ atmosphere. Briefly Transferrin Alexa Fluor 568 (2.5 μ L) (5 mg mL⁻¹) was incubated to label clathrin mediated endocytosis (CME). Dextran Alexa Fluor 568 (30 μ L) (1 mg mL⁻¹) a fluid-phase uptake marker, was used to label macropinocytosis. Cholera toxin B Alexa Fluor 594 (2.5 μ L) (10 mg mL⁻¹) to label caveolae mediated endocytosis (CvME), and LysoTracker® (50 μ L) (20 μ M) to label lysosomes. All endocytic markers were purchased from Life Technologies (Eugene, OR, USA). Next, the medium containing the complexes and the endocytic markers was removed, and cells were washed twice with PBS. Afterwards, the cells were fixed, mounted and observed under fluorescence microscopy as

described above. ImageJ software was used to quantify the colocalization of the green and red signal by a cross-correlation analysis as previously described [27].

2.7. Endosomal escape

As an analogue of the endosomal compartment, anionic micelles based on phosphatidylserine (PS) were prepared, as described previously [28]. PS was dissolved in chloroform at 1.6 mM and left under magnetic stirring until the solvent was completely evaporated. Then, PBS was added to the dried sample and a dispersed solution was obtained by sonication during 30 s at 50 w (Branson Sonifier 250, Danbury). PS micelles and the complexes were incubated at a w/w ratio of 1:50 (pCMS-EGFP: PS) for 1 h. Finally, the amount of the released DNA from each complex was determined by agarose gel electrophoresis after staining with GelRed.

2.8. Animal model

Embryonic E17.5 embryos from n = 4 Sprague Dawley rats were employed to obtain primary central nervous system cells, from the retinal tissue and brain cortex. Adult female C57BL/6 mice were used as experimental animals for subretinal, intravitreal and brain administration. All the experimental procedures were carried out in accordance with the RD 53/2013 Spanish and 2010/63/EU European Union regulations for the use of animals in scientific research. Procedures were approved and supervised by the Miguel Hernandez University Standing Committee for Animal Use in the Laboratory with code UMH.IB.EFJ.03.19/02.18.

2.9. Transfection efficiency assays of niosphingoplexes in rat primary retinal and neuronal cell cultures

The chemical dissociation of the retina tissue and brain cortex, seeding of the cells, maintenance and transfection procedures were carried out as previously described [26,29] employing niosphingoplexes. Lipofectamine™ 2000 (Invitrogen, California, USA) at 2/1 ratio

(w/w) was used as a positive control. Each condition was performed in triplicate.

2.10. Subretinal, intravitreal and brain administration

Adult C57BL/6 female mice (6–7 weeks old and 20–25 g body weight) were used as experimental animal model. Niosphingoplexes were injected in the eyes intravitreally ($n = 3$) or subretinally ($n = 3$) under an operating microscope (Zeiss OPMI® pico; Carl Zeiss Meditec GmbH, Jena, Germany) with the aid of a Hamilton microsyringe (Hamilton Co., Reno, NV), as previously described [18]. Brain administration of niosphingoplexes at cortex level were also performed in C57BL/6 mice ($n = 3$) following the procedure previously reported [29].

2.11. Evaluation of EGFP expression in mouse retina and brain

EGFP expression in mouse retina was evaluated qualitatively 1 week after the injection of niosphingoplexes in wholemount and sagittal sections of the retina, as previously described [30]. Nuclei were stained with Hoechst 33,342 (Thermo Fisher Scientific, Madrid, Spain) in frozen sections and wholemount retinas. EGFP expression in mice brains was evaluated qualitatively 1 week after surgery once the brain samples were processed, as previously described [31]. Then, the 20 μm brain slices were processed for immunohistochemistry. For blocking non-specific staining, sections were incubate in 10% BSA with 0.5% Triton in PBS for 1 h and then incubated overnight with chicken anti-GFP (Invitrogen, 1:100) diluted in PBS containing 0.5% Triton X-100. Then, sections were washed and incubated with Alexa Fluor 488-conjugated goat anti-chicken IgG (Invitrogen, 1:100) for one hour. Nuclei were stained with Hoechst 33342.

2.12. Statistical analysis

To analyze the differences between more than two groups, a 1-way ANOVA followed by Student–Newman–Keuls test was performed once normality had been proven; otherwise, the non-parametric Kruskal–Wallis test followed by a Mann–Whitney U test was used. Data were expressed as mean \pm SD. A P value ≤ 0.05 was considered statistically significant. Analyses were performed with the IBM SPSS Statistics 22.0 statistical package.

3. Results

3.1. Physicochemical characterization of formulations

The physicochemical properties of the niosphingosome and niosome formulations, as well as the corresponding complexes obtained upon the addition of plasmid DNA at cationic lipid/DNA mass ratios 3/1, 7.5/1 and 15/1, are represented in Fig. 2. The mean diameter size of niosphingosomes was 123.5 ± 12.5 . Interestingly, this value decreased slightly up to 27% after the addition of plasmid DNA at all the cationic lipid/DNA mass ratios studied (Fig. 2a, black bars). In the case of niosomes, the mean diameter size before the addition of plasmid DNA was higher, 158.9 ± 4.4 , nm and this value slightly increased to 40% at cationic lipid/DNA mass ratio 7.5/1, with no relevant changes at ratios 3/1 and 15/1 (Fig. 2a, white bars). Regarding zeta potential, all formulations showed positive values above zero, being zeta potential values of formulations containing sphingolipids higher than their counterparts. Before the addition of plasmid DNA, zeta potential of niosphingosomes and niosomes was 37.0 ± 7.8 mV and 25.0 ± 9.0 mV, respectively. In both cases, after the addition of plasmid DNA at cationic lipid/DNA mass ratio 3/1, these values declined considerably and then showed a moderate upward trend when incrementing the cationic lipid/DNA mass ratios to 7.5/1 and 15/1 (Fig. 2a, lines). The dispersity values of all samples were below 0.5 (Fig. 2b) and no relevant differences were found between both formulations, except for niosphingoplexes at cationic lipid/DNA mass ratio 3/1, which presented clearly lower PDI values (0.19 ± 0.01) than the rest of formulations. Under TEM microscopy, both sphingoniosome and niosome formulations showed a clear spherical and regular shape (Fig. 2c).

3.2. Cell viability and transfection efficiency in ARPE-19 cells

Cell viability and transfection assays were performed with niosphingoplexes and nioplexes at cationic lipid/DNA mass ratios 3/1, 7.5/1 and 15/1 in ARPE-19 cells (Fig. 3) Lipofectamine™ 2000 was employed as a positive control at 2/1 mass ratio, obtaining $39.56 \pm 1.7\%$ of live EGFP expressing cells. All data were normalized in relation to this value. As shown in Fig. 3a, niosphingoplexes at cationic lipid/DNA mass ratio 3/1 obtained the highest transfection value ($P < 0.001$), with a normalized percentage of live EGFP expressing cells of $36.7 \pm 1.6\%$ (Fig. 3a, black bars). Regarding nioplexes, transfection percentages at cationic lipid/DNA mass ratio 3/1 were clearly lower than those values obtained with niosphingoplexes, around 3%, and increased to 22% and

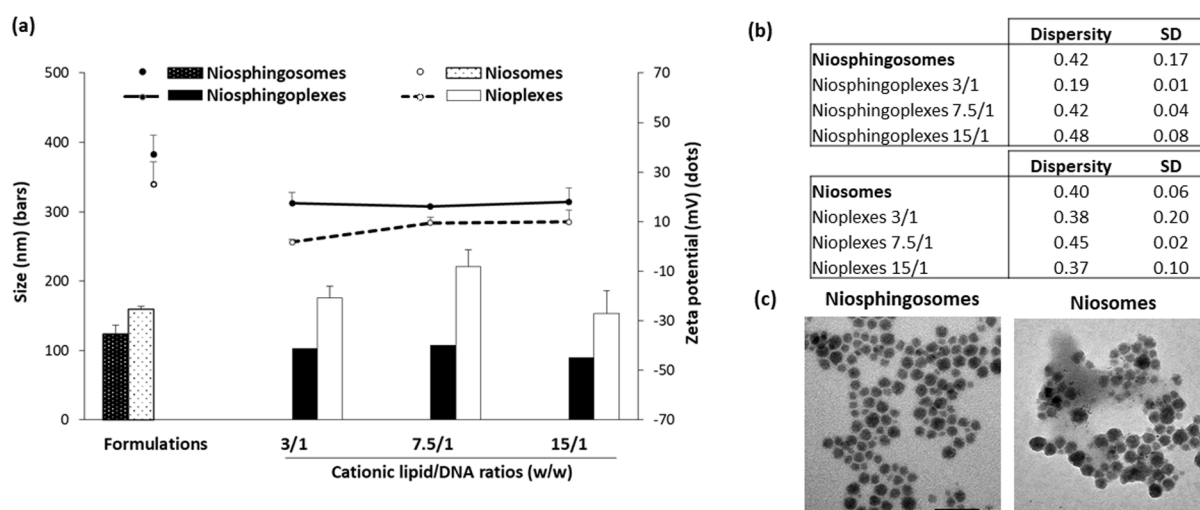


Fig. 2. Physicochemical characterization of formulations and complexes prepared with helper component (niosphingosomes/niosphingoplexes) and without helper component (niosomes/nioplexes). (a) Size (bars) and zeta potential (dots). (b) Dispersity index and standard deviation values of formulations and complexes. Each value represents the mean \pm standard deviation of three measurements. (c) TEM images of niosphingosomes and niosomes. Scale bars: 100 nm.

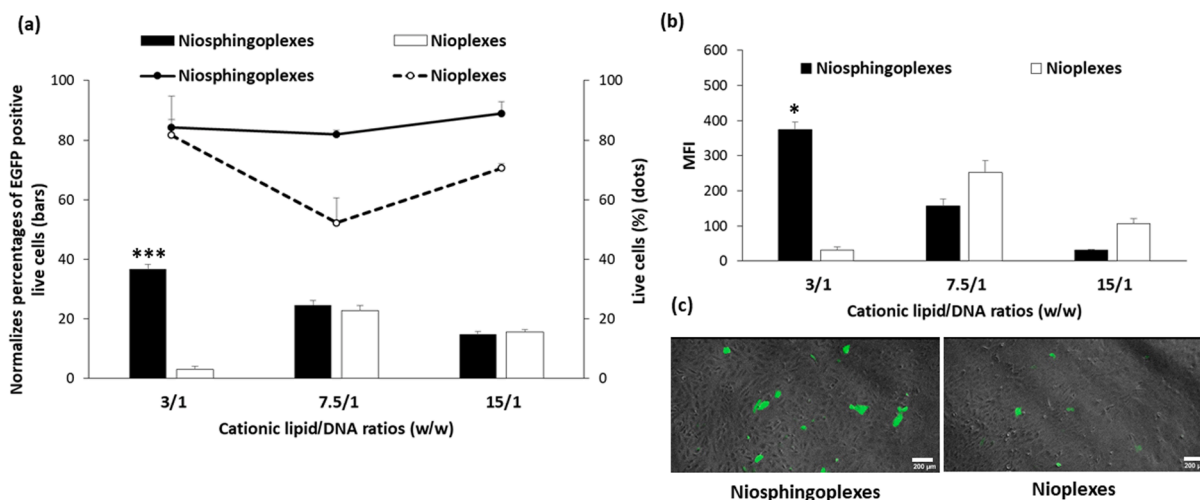


Fig. 3. Transfection efficiency and cell viability in ARPE-19 cell line 48 h post-transfection with niosphingoplexes and nioplexes. (a) Normalized percentages of transfection efficiency (bars) and cell viability (dots). (b) MFI of niosphingoplexes and nioplexes. Each value represents the mean \pm standard deviation of three measurements. (c) Overlay phase contrast images showing EGFP signals in ARPE-19 cells transfected with niosphingoplexes and nioplexes at 3/1 cationic lipid/DNA ratio (w/w). Scale bar: 200 μ m. *** $P < 0.001$; * $P < 0.05$.

to 15% when using cationic lipid/DNA mass ratios 7.5/1 and 15/1, respectively (Fig. 3a, white bars). A similar pattern was observed when the expression of the EGFP plasmid was analyzed by mean fluorescence intensity (MFI) (Fig. 3b), corroborating the highest transfection efficiency of niosphingoplexes at 3/1 cationic lipid/DNA mass ratio ($P < 0.05$). Percentages of living cells were also higher when cells were exposed to niosphingoplexes, obtaining values above 80% at all conditions. In the case of nioplexes, the percentage of living cells reached the lowest value (56%) at 7.5/1 cationic lipid/DNA mass ratio (Fig. 3a, lines). These data were further confirmed by fluorescence microscopy, where Fig. 3c shows representative images of EGFP signal in ARPE-19 cells transfected with niosphingoplexes and with nioplexes at cationic lipid/DNA mass ratio 3/1.

3.3. Cellular uptake and intracellular trafficking pathways of complexes in ARPE-19 cells

Cell uptake percentages results (Figs. 4 and 6) showed that both nioplexes and niosphingoplexes at cationic lipid/DNA mass ratio 3/1 were almost totally internalized by all the cells (more than 98%) at 2 h

and 4 h of exposition. Lipofectamine™ 2000 was employed as a positive control at 2/1 mass ratio, obtaining values around 95%. For additional uptake data, we also analyzed the mean fluorescence intensity (MFI) of the cells that internalized the complexes (Fig. 4a, dots and lines). In this case, again, niosphingoplexes and nioplexes showed similar values. However, MFI values were clearly higher for both complexes at 4 h than at 2 h after the exposition to niosphingoplexes ($P < 0.001$) or to nioplexes ($P < 0.01$). All data were normalized in relation to values obtained with Lipofectamine™ 2000 positive control at 2/1 mass ratio (95%).

Intracellular distribution studies of these formulations in ARPE-19 cells were qualitatively analyzed by representative confocal fluorescence microscopy images, showing co-localization between the intracellular trafficking pathways and the complexes (Fig. 5a). The quantitative analysis elicited that niosphingoplexes had a less participation of the CvME pathway with a 0.25 peak value of cross-correlation function (CCF) compared to both CME (0.31 CCF peak value) and macropinocytosis ($P < 0.05$; 0.42 CCF peak value), as can be observed in Fig. 5c, (black bars). However, in the case of niosome formulations, the three pathways studied exhibited a more uniform participation in

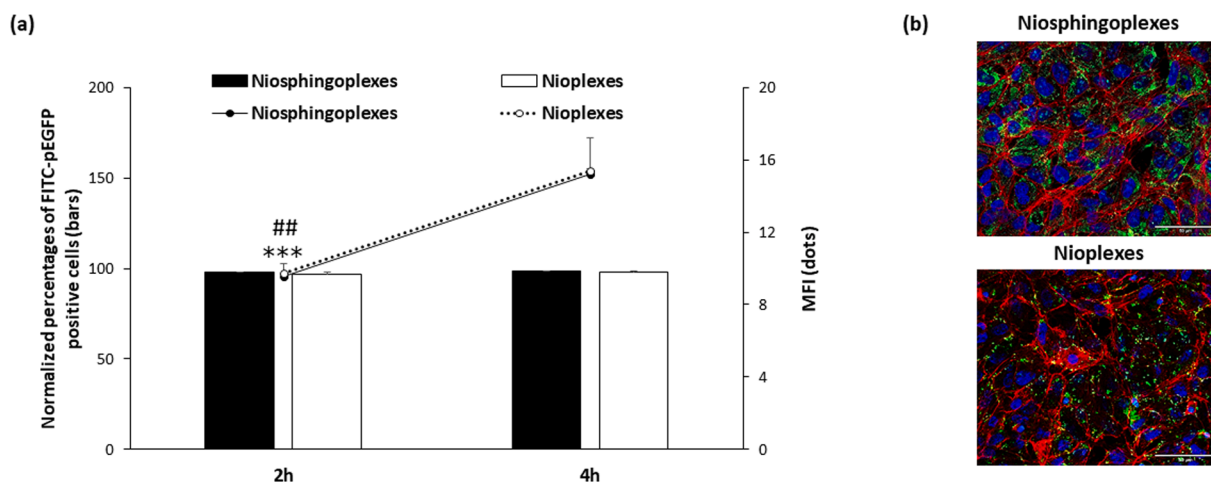


Fig. 4. Cellular uptake in ARPE-19 cell line of both niosphingoplexes and nioplexes complexes at 3/1 cationic lipid/DNA ratio (w/w). (a) Percentages of FITC-pEGFP positive cells (bars) and mean fluorescence intensity (dots) at 2 h and 4 h of exposition. Each value represents the mean \pm standard deviation of three measurements. (b) Confocal microscopy images showing the cellular uptake of complexes in ARPE-19 cells at 4 h. Cell nuclei were colored in blue (DAPI); F-actin in red (Phalloidin). Scale bar: 50 μ m. *** $P < 0.001$ for niosphingoplexes; ## $P < 0.01$ for nioplexes.

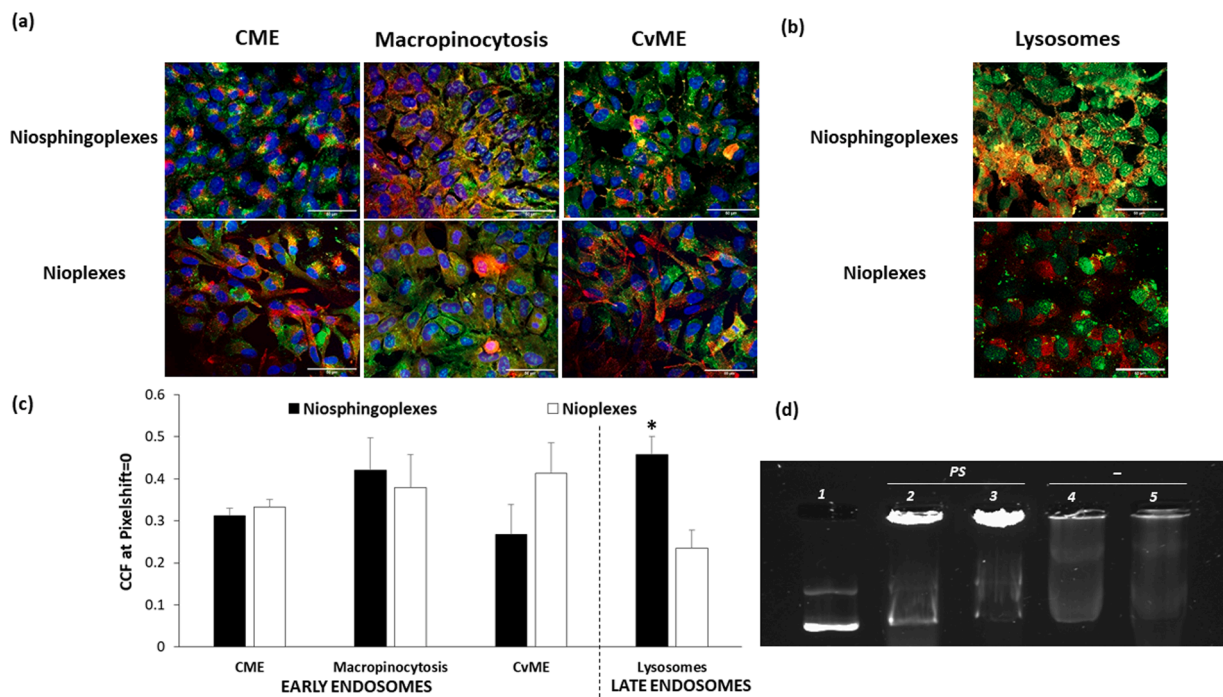


Fig. 5. Intracellular trafficking pathway assay of complexes in ARPE-19 cells. (a) Confocal microscopy merged images showing ARPE-19 cells co-incubated with complexes containing the FITC-labeled pEGFP plasmid (green) and with one of the following endocytic vesicle markers (red): Transferrin Alexa Fluor 568 for CME, Dextran Alexa Fluor 568 for macropinocytosis, and Cholera toxin B Alexa Fluor 594 for CvME. Scale bar: 50 μ m. (b) Confocal microscopy merged images showing ARPE-19 cells co-incubated with complexes containing the FITC-labeled pEGFP plasmid (green) and with Lysotracker Red-DND-99 (red) to stain the late endosome. (c) Co-localization values of red and green signals assessed by cross-correlation function (CCF) analysis in complexes. Data represent the mean \pm standard deviation of three measurements; * $P < 0.05$ for niosphingoplexes vs nioplexes. (d) DNA release profiles in agarose gel electrophoresis assay. Lane 1 naked DNA, lane 2 niosphingoplexes co-incubated with PS, lane 3 nioplexes co-incubated with PS. lane 4 niosphingoplexes, lane 5 nioplexes. PS refers to phosphatidyl serine micelles.

endocytosis process. CCF peak value was 0.35 for CME, 0.38 for macropinocytosis, and 0.41 for CvME (Fig. 5c, white bars). Additionally, the co-localization of the complexes with lysosomes was also evaluated. In this case, niosphingoplexes exhibited a higher and statistically significant ($P < 0.05$) co-localization value (0.45 ± 0.03 CCF peak value) compared to niosomes (0.23 ± 0.05 CCF peak value). A representative fluorescence image obtained by confocal microscopy of the co-localization between complexes and lysosomes is shown in Fig. 5b. Interestingly, the co-incubation of the complexes with the PS micelles, that resemble the late endosome compartment, in an agarose gel assay showed that DNA incorporated in niosphingosomes was more efficiently released from the micelles (Fig. 5d, lane 2) than DNA bound to niosomes (Fig. 5d, lane 3).

3.4. *In vivo* transfection efficiency of niosphingoplexes in mice retina and brain

In vivo preliminary studies were carried out to evaluate the capacity of niosphingoplexes to deliver the EGFP into the mice retinas after both subretinal (Fig. 6a) and intravitreal (Fig. 6b) injections. Data revealed that EGFP expression was present in several retinal layers including outer segments of photoreceptors, outer plexiform layer, inner plexiform layer and ganglion cell layer where some end-foot of the Müller glia cells (red colour) co-localized with EGFP after subretinal and intravitreal administration of niosphingoplexes. Additionally, EGFP expression was also present in the cytoplasmic extensions of cortical cells of the mice brains in the superficial region of the cerebral cortex injected area (Fig. 6c).

4. Discussion

Sphingolipids are amphiphilic biomolecules, with a polar terminal group (OH) and a hydrocarbon chain. When amphiphilic molecules are

dispersed in water, they can spontaneously organize themselves into colloidal vesicles [32], which can enhance the drug delivery capacity of such system. Besides, sphingolipids have desirable physicochemical properties that can stabilize the emulsions, since their surface-active wetting capacity can coat the surface of crystals to enhance the hydrophilicity of hydrophobic drugs [33]. In addition to all of the above-mentioned properties, sphingosine, and sphingosine-1-phosphate among other sphingolipids metabolites, attract attention as bioactive signaling molecules engaged in the regulation of cell metabolism processes, such as cell growth, differentiation, senescence, and apoptosis [34], by modifying the properties of cell membranes [35]. Such sphingosine can be found in the sphingolipids extract obtained from animal origin, which show a more suitable profile to obtain ceramides [21].

In this study, we incorporated sphingolipids from animal origin as “helper” component into niosome formulations, in order to evaluate the biophysical properties as gene delivery system. The physicochemical characterization results (Fig. 2) showed that all formulations showed positive charge values, which is required to prevent the formation of aggregates due to the electrostatic interactions [16]. Moreover, all formulations and complexes presented particle sizes in the nanoscale range, suitable for gene delivery purposes [36]. The incorporation of sphingolipids as “helper” component into the cationic niosome formulation decreased particle size. Interestingly, such differences in particle size were not only maintained but also decreased when the formulations were complexed with the EGFP plasmid. Additionally, compared to niosphingosomes, niosphingoplexes had a smaller particle size at all cationic lipid/DNA mass ratios studied, probably by due to the additional electrostatic interactions between the cationic niosphingosomes and the anionic plasmid DNA [15,36]. In fact, regarding superficial charge, the presence of sphingolipid amphiphilic biomolecules in the composition of niosomes increased zeta potential, and this higher zeta potential was maintained also at all the cationic lipid/DNA mass ratios

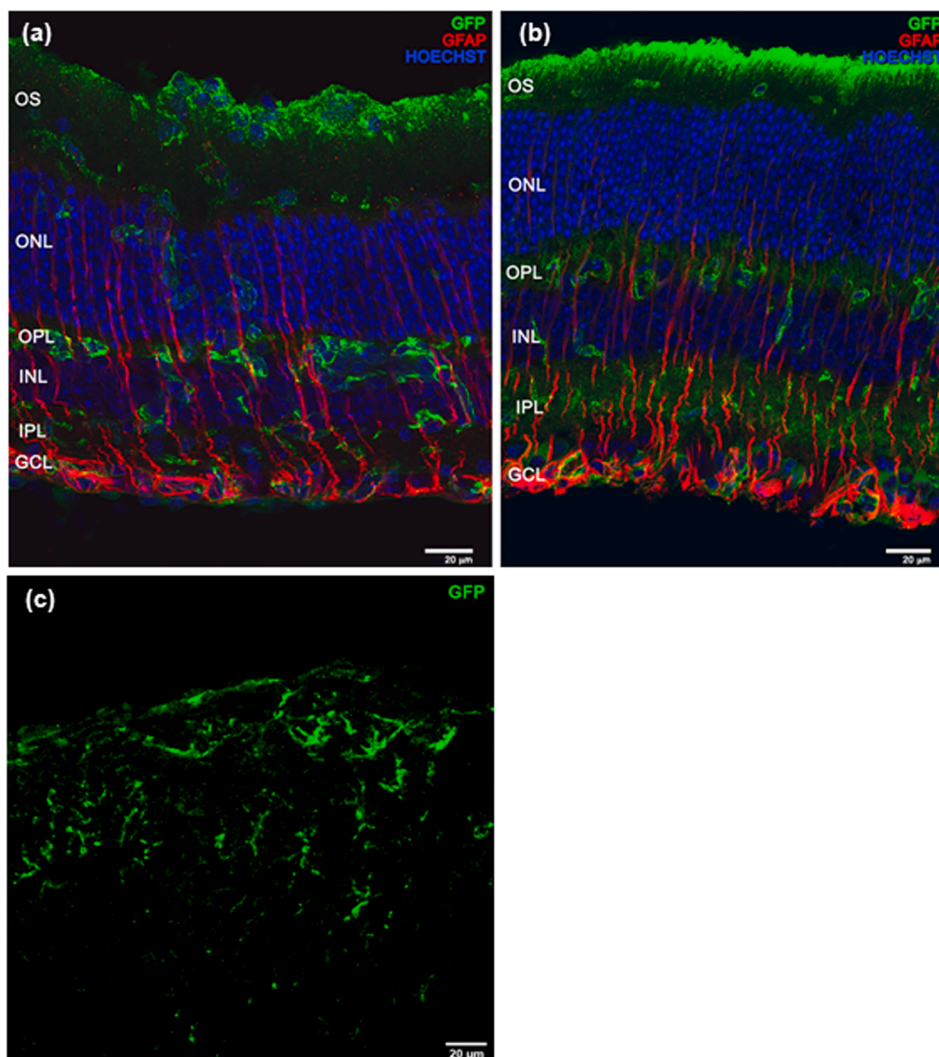


Fig. 6. *In vivo* immunohistochemistry gene expression of EGFP (green) in frozen sections one week after subretinal (a), intravitreal (b) and cerebral cortex (c) injections of niosphingoplexes at 3/1 cationic lipid/DNA ratio (w/w). Scale bar: 20 μm . OS, outer segments; ONL outer nuclear layer; OPL outer plexiform layer; INL inner nuclear layer; IPL inner plexiform layer; GCL ganglion cell layer.

studied. Regarding the dispersity index, niosphingoplexes at cationic lipid/DNA mass ratio 3/1 showed the lowest value of this parameter (0.19 ± 0.01), which point out that at this condition a better homogeneity of complexes is obtained. Additionally, niosphingosomes presented a clear spherical and homogeneous morphology under TEM examination, without aggregations, probably due to the electrostatic repulsion among highly positive charged particles.

Once the formulations were characterized in physicochemical terms we performed *in vitro* gene delivery studies with niosphingoplexes and nioplexes at cationic lipid/DNA mass ratios 3/1, 7.5/1 and 15/1 in ARPE-19 cell line, since these cells play an important role in retinal diseases [15]. Moreover, ARPE-19 cell is a well recognized retinal cell model to evaluate gene transfection efficiency. Interestingly, although niosphingoplexes with different cationic lipid/DNA ratios showed similar size and zeta potential values in previously conducted physicochemical studies, they reported statistical differences in terms of transfection efficiency and cell viability, which reveals the complexity of the transfection process. In particular, we observed that niosphingoplexes at cationic lipid/DNA mass ratio 3/1 reached the highest percentage of transfected cells ($P < 0.001$) compared to the rest of conditions. In parallel, MFI analysis was also analyzed to evaluate not only the percentage of live cells transfected, but also the intensity of the fluorescence signal, which is close related to the quantity of protein expressed after

the transfection process. Such MFI studies also revealed that the highest intensity value was reached when ARPE-19 cells were treated with niosphingoplexes at 3/1 cationic lipid/DNA mass ratio. All in all, data obtained from transfection efficiency experiments suggest that at 3/1 cationic lipid/DNA mass ratio, the presence of sphingolipid biomolecules in the niosome composition not only increases the percentage of transfected cells, but also the quantity of protein expressed in such transfected cells [15], which can have critical clinical relevance. Interestingly, data obtained from the transfection experiments also revealed that niosphingoplexes at all cationic lipid/DNA mass ratios had higher cell viability values (above 80% in ARPE-19 cells), than their niosome counterparts, which points out the biocompatibility effect that the incorporation of sphingolipids has into the niosome formulation. This biocompatibility of niosphingoplexes was also confirmed, qualitatively, by the healthy appearance of ARPE-19 cells under fluorescence microscope examination 48 h after transfection. By contrast, the transfection positive control Lipofectamine™ 2000 showed low cell viability values, below 65% (data not shown), revealing the toxicity associated to such commercial formulation, which hampers its clinical application [27]. In terms of clinical applications, it is also important to highlight that the best transfection efficiency with high cell viability was obtained when ARPE-19 cells were exposed to niosphingoplexes at the lowest cationic lipid/DNA ratio of 3/1. Such achievement would allow a higher gene

loading capacity in small injection volumes that normally are required to face devastating pathologies of both *brain and retina*, by means of gene therapy approach.

To further evaluate the impact that the incorporation of sphingolipid biomolecules has on the transfection process we performed also a cellular uptake study, since this parameter can drastically affect to the transfection efficiency [15]. However, our cellular uptake studies revealed that there were no difference in the cellular uptake of both formulations, in terms of both percentage of cells that internalized the complexes and quantity of particles that were internalized in cells. In any case, the internalization process was more efficient when cells were exposed to formulations during 4 h instead of 2 h. These data suggest the relevance that the kinetic of the internalization process has on the transfection efficiency, although in this case, there were *no* differences observed between niosphingoplexes and niosome formulations. Therefore, we also studied other biological parameters such as the intracellular trafficking process of both formulations to further explore the influence that the integration of sphingolipids in niosome composition has on the transfection process [37].

Intracellular trafficking studies were carried out to analyse the co-localization of the formulations with the most employed endocytosis pathways present in ARPE-19 cells such as CvME, CME and macropinocytosis [38,39]. Our data revealed that the highest difference between both formulations was found in the CvME pathway. This endocytic pathway was minority in the case of niosphingoplexes formulation, which in fact preferred the macropinocytosis pathway, while niosomes were equally internalized by the three endocytosis pathways studied. Therefore, our data suggest that the presence of sphingolipids might turn the internalization mechanism of niosphingoplexes from CvME to macropinocytosis endocytic pathway. In this sense, it has been described that macropinocytosis is implicated in the internalization of cell penetrating peptides and proteins into cells [40,41]. Moreover, co-localization studies in the late endosomal compartment were also conducted. In this case, niosphingoplexes co-localized with lysosomes in a higher rate than nioplexes (Fig. 5c). It has been suggested that there is a suppression of lysosomal activity when complexes enter into ARPE-19 cells by CvME, and that such complexes are located around the nucleus, which hampers the release of DNA from the complexes [39]. This suggestion supports our results, since compared to niosphingoplexes, nioplexes (that showed less transfection efficiency) entered into the cell mainly via CvME, with the consequent lack of lysosomal activity. Another critical parameter that clearly impact on transfection process of complexes designed for gene delivery is the *endosomal escape*. Some nucleic acid delivery systems failed to achieve good levels of transfection efficiencies, despite being efficiently internalized into the cells, due to their poor of endosomal escape performance [42]. Thus, we next elaborated anionic micelles based on PS to evaluate the release of the complexed plasmid DNA from the late endosomes and avoid lysosomal degradation. As observed in Fig. 5d, a small amount of plasmid was released from niosphingoplexes (lane 2), and no release of plasmid was observed from the nioplexes (lane 3) in the agarose gel electrophoresis assay. Such data suggest that the incorporation of sphingolipids into the cationic niosome formulation could provide endosomal escape properties to the complexes, which in fact could contribute to increase transfection efficiency. Another biological barrier that hampers transfection process is the nuclear membrane. In this sense, and taking into account the crucial signaling and regulatory roles that sphingolipids have in the nucleus [43], it is likely that such sphingolipids could be promoting gene delivery by a regulatory mechanism in the cell nucleus. Recent findings concerning nuclear sphingolipids found that different kind of sphingolipids have particular nuclear functions by temporally and spatially specific mechanisms. For example, sphingomyelin is involved in the structure and regulation of chromatin architecture, DNA synthesis and RNA stability, while sphingosine acts as ligand for the nuclear receptor steroidogenic factor 1 regulating gene transcription; and sphingosine-1-phosphate regulates gene expression

epigenetically by histone acetylation [44].

Before performing *in vivo* experiments, we made a proof of concept assay to evaluate if niosphingoplexes at cationic lipid/DNA mass ratio 3/1 (w/w) were able to deliver the EGFP plasmid in an efficient way to both rat embryonal retinal and cerebral cortex primary cells. Our results (Supplementary material) revealed EGFP expression in both retinal (Fig. S1a) and cortical (Fig. S1c) primary cells evaluated 72 h after transfection.

Therefore, motivated by those results, niosphingoplexes were implemented in *in vivo* studies to assess their capacity to deliver the genetic material to mouse retina, after both intravitreal and subretinal injection, and to mouse brain, after administration of niosphingoplexes at the cortex level. Because of their relevant physiological function, both brain and eye are immune-privileged sites isolated from the rest of the organism by additional extracellular barriers such the BBB and the BRB [45,46]. An ideal scenario would contemplate the delivery of genetic material by a safe and efficient non-viral vector to immune-privileged sites through non-invasive administration routes, such as the topical instillation in the cornea that circumvent the BRB to reach the retina, and the nose-to-brain administration to access directly into the brain bypassing the BBB [47]. However, at present, this possibility is far away to be applied into the regular medical practice to face by gene therapy devastating diseases that affect the brain and retina. Therefore, we evaluated the local administration of niosphingoplexes in retina and brain. In the case of the eye, the most employed administration routes to reach the retina at a clinical level include the intravitreal and subretinal injection [18]. Our data revealed that after intravitreal and subretinal injections, EGFP expression was present in several layers and cells of the retina. More specifically, EGFP expression was observed mainly in the outer segments of photoreceptors, outer plexiform layer, and in the inner plexiform layer, where some end-foot of the Müller glia cells exhibited green fluorescence signal. Gene delivery to the outer layers of the retina is of utmost importance from a therapeutic standpoint, since there have been described more than 200 gene mutations at this level, related to relevant pathologies of the retina such as Stargardt disease, retinitis pigmentosa, or Leber's congenital amaurosis, to name just the most relevant ones [17]. On the other hand, transfection of ganglion cell layer in the retina has relevance to face glaucoma disease where these cells are affected [48]. Interestingly, in the case of brain administration at the cortex level, we also found EGFP expression in the cytoplasmic extensions of cortical cells, close to the injection site. This area of the brain is usually affected in devastating diseases of the central nervous systems, such as epilepsy, Alzheimer's and Parkinson's diseases, leading to relevant perturbation and neurological disorders [49,50]. Therefore, our preliminary proof of concept *in vivo* assay shows promising results to deliver in the future therapeutic genetic material into the retina and brain of animal models that resembles human diseases of these relevant and immune-privileged tissues.

5. Conclusions

Overall, this manuscript points out the biophysical properties of sphingolipid extracts from animal origin for gene delivery purposes when they are incorporated into cationic niosomes. Such biomaterial impacts not only on relevant physicochemical properties of cationic niosomes that influence on transfection efficiency, such as particle size or zeta potential, but also in biological properties, such as their intracellular disposition or endosomal escape properties. Moreover, our proof of concept *in vivo* results suggest that niosphingosomes represent a promising non-viral vector biomaterial for the treatment of both retinal and brain diseases by gene therapy approach.

Declaration of Competing Interest

The authors declare that they have no known competing financial interests or personal relationships that could have appeared to influence

the work reported in this paper.

Acknowledgements

This work was supported by the Basque Country Government (Department of Education, University and Research, Consolidated Groups IT907-16). Additional funding was provided by the CIBER of Bioengineering, Biomaterials and Nanomedicine (CIBER-BBN), an initiative of the Carlos III Health Institute (ISCIII). I.V.B. and M.S.R. thank the University of the Basque Country (UPV/EHU) for the granted postdoctoral fellowship (ESPDOC19/47) and the granted pre-doctoral fellowship (PIF17/79), respectively. Authors wish to thank the intellectual and technical assistance from the ICTS “NANBIOSIS,” more specifically by the Drug Formulation Unit (U10) of the CIBER in Bioengineering, Biomaterials and Nanomedicine (CIBER-BBN) at the University of Basque Country (UPV/EHU). Technical and human support provided by SGIKER (UPV/EHU) is also gratefully acknowledged.

Appendix A. Supplementary data

Supplementary data to this article can be found online at <https://doi.org/10.1016/j.ejpb.2021.09.011>.

References

- [1] C.E. Dunbar, K.A. High, J.K. Joung, D.B. Kohn, K. Ozawa, M. Sadelain, Gene Therapy Comes of Age, *Science* 359 (6372) (2018), eaan4672, <https://doi.org/10.1126/science.aan4672>.
- [2] A. Mullard, Gene Therapy Boom Continues, *Nat. Rev. Drug Discov.* 18 (2019), 737–019-00154-0.
- [3] Y.K. Sung, S.W. Kim, Recent Advances in the Development of Gene Delivery Systems, *Biomater. Res.* 23 (2019), 8–019-0156-z eCollection 2019.
- [4] S. Ingusci, G. Verlengia, M. Soukupova, S. Zucchini, M. Simonato, Gene Therapy Tools for Brain Diseases, *Front. Pharmacol.* 10 (2019) 724.
- [5] J.W. Streilein, Ocular Immune Privilege: Therapeutic Opportunities from an Experiment of Nature, *Nat. Rev. Immunol.* 3 (2003) 879–889.
- [6] E.E. Vaughan, J.V. DeGiulio, D.A. Dean, Intracellular Trafficking of Plasmids for Gene Therapy: Mechanisms of Cytoplasmic Movement and Nuclear Import, *Curr. Gene Ther.* 6 (2006) 671–681.
- [7] N. Nayerossadat, T. Maedeh, P.A. Ali, Viral and Nonviral Delivery Systems for Gene Delivery, *Adv. Biomed. Res.* 1 (2012), 9175.98152. Epub 2012 Jul 6.
- [8] M. Foldvari, D.W. Chen, N. Nafissi, D. Calderon, L. Narsineni, A. Rafiee, Non-Viral Gene Therapy: Gains and Challenges of Non-Invasive Administration Methods, *J. Control. Release* 240 (2016) 165–190.
- [9] D. Zhi, Y. Bai, J. Yang, S. Cui, Y. Zhao, H. Chen, S. Zhang, A Review on Cationic Lipids with Different Linkers for Gene Delivery, *Adv. Colloid Interface Sci.* 253 (2018) 117–140.
- [10] E. Ojeda, G. Puras, M. Agirre, J. Zárate, S. Grijalvo, R. Pons, R. Eritja, G. Martínez-Navarrete, C. Soto-Sánchez, E. Fernández, J.L. Pedraz, Niosomes based on synthetic cationic lipids for gene delivery: the influence of polar head-groups on the transfection efficiency in HEK-293, ARPE-19 and MSC-D1 cells, *Org. Biomol. Chem.* 13 (4) (2015) 1068–1081.
- [11] M. Riley, W. Vermeris, Recent Advances in Nanomaterials for Gene Delivery-A Review, *Nanomaterials (Basel)* 7 (5) (2017) 94, <https://doi.org/10.3390/nano7050094>.
- [12] G. Puras, M. Mashal, J. Zárate, M. Agirre, E. Ojeda, S. Grijalvo, R. Eritja, A. Diaz-Tahoces, G. Martínez Navarrete, M. Avilés-Trigueros, E. Fernández, J.L. Pedraz, A novel cationic niosome formulation for gene delivery to the retina, *J. Control Release* 28 (174) (2014 Jan) 27–36.
- [13] S. Grijalvo, G. Puras, J. Zárate, M. Sainz-Ramos, N.A.L. Qtaish, T. López, M. Mashal, N. Attia, D. Díaz, R. Pons, E. Fernández, J.L. Pedraz, R. Eritja, Cationic Niosomes as Non-Viral Vehicles for Nucleic Acids: Challenges and Opportunities in Gene Delivery, *Pharmaceutics* 11 (2) (2019) 50.
- [14] R. Bartelds, M.H. Nematollahi, T. Pols, M.C.A. Stuart, A. Pardakhty, G. Asadikaram, B. Poolman, Z. Leonenko, Niosomes, an Alternative for Liposomal Delivery, *PLoS ONE* 13 (4) (2018), e0194179.
- [15] E. Ojeda, G. Puras, M. Agirre, J. Zarate, S. Grijalvo, R. Eritja, L. DiGiacomo, G. Caracciolo, J.L. Pedraz, The Role of Helper Lipids in the Intracellular Disposition and Transfection Efficiency of Niosome Formulations for Gene Delivery to Retinal Pigment Epithelial Cells, *Int. J. Pharm.* 503 (2016) 115–126.
- [16] E. Ojeda, G. Puras, M. Agirre, J. Zarate, S. Grijalvo, R. Eritja, G. Martínez-Navarrete, C. Soto-Sánchez, A. Diaz-Tahoces, M. Avilés-Trigueros, E. Fernández, J. L. Pedraz, The influence of the polar head-group of synthetic cationic lipids on the transfection efficiency mediated by niosomes in rat retina and brain, *Biomaterials* 77 (2016) 267–279.
- [17] M. Mashal, N. Attia, G. Puras, G. Martínez-Navarrete, E. Fernández, J.L. Pedraz, Retinal Gene Delivery Enhancement by Lycopene Incorporation into Cationic Niosomes Based on DOTMA and Polysorbate 60, *J. Control. Release* 254 (2017) 55–64.
- [18] M. Mashal, N. Attia, G. Martínez-Navarrete, C. Soto-Sánchez, E. Fernández, S. Grijalvo, R. Eritja, G. Puras, J.L. Pedraz, Gene Delivery to the Rat Retina by Non-Viral Vectors Based on Chloroquine-Containing Cationic Niosomes, *J. Control. Release* 304 (2019) 181–190.
- [19] J. Chun, H.P. Hartung, Mechanism of Action of Oral Fingolimod (FTY720) in Multiple Sclerosis, *Clin. Neuropharmacol.* 33 (2010) 91–101.
- [20] H. Alrbyawi, I. Poudel, R.P. Dash, N.R. Srinivas, A.K. Tiwari, R.D. Arnold, R. J. Babu, Role of Ceramides in Drug Delivery, *AAPS Pharm. Sci. Tech.* 20 (2019), 287–019-1497-6.
- [21] S. Cerrato, L. Ramió-Lluch, P. Brazis, D. Fondevila, S. Segarra, A. Puigdemont, Effects of sphingolipid extracts on the morphological structure and lipid profile in an in vitro model of canine skin, *Vet. J.* 212 (2016) 58–64.
- [22] R. Dahiya, T.A. Brasitus, Distribution of glycosphingolipids and ceramide of rat small intestinal mucosa, *Lipids* 21 (2) (1986) 112–116.
- [23] E.N. Tessema, T. Gebre-Mariam, G. Paulos, J. Wohlrab, R.H.H. Neubert, Delivery of Oat-Derived Phytoceramides into the Stratum Corneum of the Skin using Nanocarriers: Formulation, Characterization and in Vitro and Ex-Vivo Penetration Studies, *Eur. J. Pharm. Biopharm.* 127 (2018) 260–269.
- [24] E. Yilmaz, H.H. Borchert, Design of a Phytosphingosine-Containing, Positively-Charged Nanoemulsion as a Colloidal Carrier System for Dermal Application of Ceramides, *Eur. J. Pharm. Biopharm.* 60 (2005) 91–98.
- [25] S.N. Park, M.H. Lee, S.J. Kim, E.R. Yu, Preparation of Quercetin and Rutin-Loaded Ceramide Liposomes and Drug-Releasing Effect in Liposome-in-Hydrogel Complex system, *Biochem. Biophys. Res. Commun.* 435 (3) (2013) 361–366.
- [26] M. Sainz-Ramos, I. Villate-Beitia, I. Gallego, N. A.L. Qtaish, T.B. Lopez-Mendez, R. Eritja, S. Grijalvo, G. Puras, J.L. Pedraz, Non-viral mediated gene therapy in human cystic fibrosis airway epithelial cells recovers chloride channel functionality, *Int. J. Pharm.* 588 (2020) 119757, <https://doi.org/10.1016/j.ijpharm.2020.119757>.
- [27] I. Villate-Beitia, I. Gallego, G. Martínez-Navarrete, J. Zárate, T. López-Méndez, C. Soto-Sánchez, E. Santos-Vizcaíno, G. Puras, E. Fernández, J.L. Pedraz, Polysorbate 20 non-ionic surfactant enhances retinal gene delivery efficiency of cationic niosomes after intravitreal and subretinal administration, *Int. J. Pharm.* 550 (1–2) (2018) 388–397.
- [28] M. Agirre, E. Ojeda, J. Zarate, G. Puras, S. Grijalvo, R. Eritja, G. García del Caño, S. Barrondo, I. González-Burguera, M. López de Jesús, J. Sallés, J.L. Pedraz, New Insights into Gene Delivery to Human Neuronal Precursor NT2 Cells: A Comparative Study between Lipoplexes, Nioplexes, and Polyplexes, *Mol. Pharm.* 12 (11) (2015) 4056–4066.
- [29] I. Gallego, I. Villate-Beitia, C. Soto-Sánchez, M. Menéndez, S. Grijalvo, R. Eritja, G. Martínez-Navarrete, L. Humphreys, T. López-Méndez, G. Puras, E. Fernández, J. L. Pedraz, Brain Angiogenesis Induced by Nonviral Gene Therapy with Potential Therapeutic Benefits for Central Nervous System Diseases, *Mol. Pharm.* 17 (6) (2020) 1848–1858.
- [30] I. Gallego, I. Villate-Beitia, G. Martínez-Navarrete, M. Menéndez, T. López-Méndez, C. Soto-Sánchez, J. Zárate, G. Puras, E. Fernández, J.L. Pedraz, Non-viral vectors based on cationic niosomes and minicircle DNA technology enhance gene delivery efficiency for biomedical applications in retinal disorders, *Nanomedicine* 17 (2019) 308–318.
- [31] C. Soto-Sánchez, G. Martínez-Navarrete, L. Humphreys, G. Puras, J. Zarate, J. L. Pedraz, E. Fernández, Enduring high-efficiency in vivo transfection of neurons with non-viral magnetoparticles in the rat visual cortex for optogenetic applications, *Nanomedicine* 11 (4) (2015) 835–843.
- [32] A. Margineanu, in: *Biological Applications of Nanoparticles in Optical Microscopy* Polymeric Nanomaterials in Nanotherapeutics, Elsevier, 2019, pp. 469–495.
- [33] J. Li, X. Wang, T. Zhang, C. Wang, Z. Huang, X. Luo, Y. Deng, A Review on Phospholipids and their Main Applications in Drug Delivery Systems, *Asian J. Pharmaceutical Sci.* 10 (2) (2015) 81–98.
- [34] N. Bartke, Y.A. Hannun, Bioactive sphingolipids: metabolism and function, *J. Lipid Res.* 50 (2009) S91–S96.
- [35] F.M. Goñi, A. Alonso, Biophysics of sphingolipids I. Membrane properties of sphingosine, ceramides and other simple sphingolipids. *Biochimica et Biophysica Acta (BBA) - Biomembranes* 1758 (12) (2006) 1902–1921.
- [36] I. Villate-Beitia, G. Puras, C. Soto-Sánchez, M. Agirre, E. Ojeda, J. Zarate, E. Fernandez, J.L. Pedraz, Non-viral vectors based on magnetoplexes, lipoplexes and polyplexes for VEGF gene delivery into central nervous system cells, *Int. J. Pharm.* 521 (2017) 130–140.
- [37] S.A. Wissing, O. Kayser, R.H. Müller, Solid lipid nanoparticles for parenteral drug delivery, *Adv. Drug. Deliv. Rev.* 56 (9) (2004) 1257–1272.
- [38] D. Manzanares, V. Ceña, Endocytosis: The Nanoparticle and Submicron Nanocompounds Gateway into the Cell, *Pharmaceutics* 12 (4) (2020 Apr 17) 371.
- [39] D. Delgado, A. del Pozo-Rodríguez, M.Á. Solinís, A. Rodríguez-Gascón, Understanding the mechanism of protamine in solid lipid nanoparticle-based lipofection: the importance of the entry pathway, *Eur. J. Pharm. Biopharm.* 79 (3) (2011) 495–502.
- [40] A.T. Jones, searching for an endocytic identity and role in the uptake of cell penetrating peptides, *J. Cell. Mol. Med.* 11 (4) (2007) 670–684.
- [41] J.P. Lim, P.A. Gleeson, Macropinocytosis: an endocytic pathway for internalising large gulps, *Immunol. Cell. Biol.* 89 (8) (2011) 836–843.
- [42] Liang, W. and Jenny K W Lam. “Endosomal Escape Pathways for Non-Viral Nucleic Acid Delivery Systems.”, 2012.
- [43] R.W. Ledeen, G. Wu, Nuclear sphingolipids: metabolism and signaling, *J. Lipid Res.* 49 (6) (2008 Jun) 1176–1186.

- [44] N.C. Lucki, M.B. Sewer, Nuclear Sphingolipid Metabolism, *Annu. Rev. Physiol.* 74 (1) (2012) 131–151.
- [45] A.M. O'Mahony, B.M. Godinho, J.F. Cryan, C.M. O'Driscoll, Non-Viral Nanosystems for Gene and Small Interfering RNA Delivery to the Central Nervous System: Formulating the Solution, *J. Pharm. Sci.* 102 (2013) 3469–3484.
- [46] Y. Zhang, F. Schlachetzki, J.Y. Li, R.J. Boado, W.M. Pardridge, Organ-specific gene expression in the rhesus monkey eye following intravenous non-viral gene transfer, *Mol. Vis.* 3 (9) (2003 Oct) 465–472.
- [47] N. Al Qtaish, I. Gallego, I. Villate-Beitia, M. Sainz-Ramos, T.B. López-Méndez, S. Grijalvo, R. Eritja, C. Soto-Sánchez, G. Martínez-Navarrete, E. Fernández, G. Puras, J.L. Pedraz, Niosome-Based Approach for In Situ Gene Delivery to Retina and Brain Cortex as Immune-Privileged Tissues, *Pharmaceutics*. 12 (3) (2020 Feb 25) 198.
- [48] G. Puras, G. Martínez-Navarrete, M. Mashal, J. Zárate, M. Agirre, E. Ojeda, S. Grijalvo, R. Eritja, A. Diaz-Tahoces, M. Avilés-Trigueros, E. Fernández, J. L. Pedraz, Protamine/DNA/Niosome Ternary Nonviral Vectors for Gene Delivery to the Retina: The Role of Protamine, *Mol. Pharm.* 12 (10) (2015) 3658–3671.
- [49] B.A. Barres, The mystery and magic of glia: a perspective on their roles in health and disease, *Neuron* 60 (3) (2008) 430–440.
- [50] E.D. Milligan, L.R. Watkins, Pathological and protective roles of glia in chronic pain, *Nat. Rev. Neurosci.* 10 (1) (2009) 23–36.